Journal of Manufacturing Processes 34 (2018) 477–485

Contents lists available at ScienceDirect

Journal of Manufacturing Processes

journal homepage: www.elsevier.com/locate/manpro

# A study of the behavior and effects of nitrogen take-up from protective gas shielding in laser welding of stainless steel

S.K. Wu[a], K. Zheng[c], J.L. Zou[a,*], F. Jiang[b], X.H. Han[c]

[a] Institute of Laser Engineering, Beijing University of Technology, Beijing, 100124, China
[b] College of Mechanical Engineering and Applied Electronics Technology, Beijing University of Technology, Beijing, 100124, China
[c] CRRC QingDao SiFang Co., LTD, Qingdao, Shangdong, 266111, China

ARTICLE INFO

*Keywords:*
Laser welding
Nitrogen shielding gas
Austenite stainless steel
Microstructure
Notch tensile
Corrosion

ABSTRACT

In this study, the SUS301l austenitic stainless steel plates were welded under different protective conditions with different percentages of $N_2$/Ar. The welded joints, that were produced using fiber laser welding and $CO_2$ laser welding, showed good shape and there were no significant differences in microstructure under different protective conditions. The welds consisted of γ-austenite and small amounts of δ-ferrite, and the welded joints were of approximately equal to the base metal in terms of their tensile strength and micro-hardness. The nitrogen that was absorbed by the molten pool mainly was concentrated around the surface of the weld and was present in the form $Cr_2N$, CrN and FeN. With an increase of the $N_2$ percentages in the protective gas, the anti-corrosion performance of the welds was improved. Compared with the fiber laser welding, the weld after $CO_2$ laser welding had a slightly higher nitrogen content and better corrosion resistance.

## 1. Introduction

Stainless steels now have been extensively applied in many industries mainly including rail transportation, energy, heavy chemical and aerospace because of their anti-corrosion properties, high-temperature resistance and good mechanical properties [1]. Currently, resistance spot welding, full-automatic or semi-automatic tungsten inert gas (TIG) welding, metal inert-gas (MIG) welding and metal-active gas arc (MAG) welding commonly are used in welding and manufacturing of stainless steel components. However, these welding technologies have many shortcomings, such as low welding efficiency and high thermal deformation [2–4]. By contrast, laser welding possesses many advantages, such as rapid weld processing, high-quality weld jointing and the production of well-formed welds, and hence the technique increasingly is used in the welding of stainless steels [5]. During the laser welding process, plasma or plume produced during metal evaporation can impose negative effects on welding stability and energy coupling [6]. Therefore, side blowing of He or Ar often is employed to control the plasma/plume and to protect the molten weld pool [7]. Helium is characterized by high ionization energy and favorable thermal conductivity and has optimal protection performances. However, helium is quite expensive. although lower in cost, heavy use of argon in industrial applications still results in serious expenditure. In consequence, the exploration of more economic protection methods of laser welding of stainless steel is of great technical and economic significance and industrial application values.

$N_2$ is the major constituent of air, with a volume fraction of up to 78.08%. $N_2$ also is simple to collects and is extremely low cost. Moreover, $N_2$ is a relatively inert diatomic gas. Compared with He, $N_2$ has almost equal ionization energy but has a larger relative atomic mass. Accordingly, the use of $N_2$ as a protective gas can control the effects of plasma/plume in laser welding process very effectively [8]. However, in conventional arc welding processes, a large amount of N is dissolved in the high-temperature molten pool. Part of nitrogen exists in solid solution in an oversaturated form during the subsequent cooling process. Nitrogen also was precipitated in the grains or at the grain boundaries in the form of $Fe_4N$, thereby reducing the plasticity and toughness of the weld metal. especially at lower temperatures [9,10]. Additionally, oversaturated nitrogen gradually precipitates during the aging process to form stable needle-shaped $Fe_4N$, which leads to age-induced embrittlement of the weld metal. When arc welding, therefore, nitrogen, as an impurity element, should be strictly controlled [11]. On the other hand, a trace amount of dissolved nitrogen in the molten pool serves as the alloying element in austenitizing, which can improve the anti-corrosion, fatigue resistance, yield and tensile performances of stainless steel and can enhance the overall mechanical properties of the welds [12]. Bhatt et al used 5% and 10% $N_2$ as the protective gas during GAT welding of duplex stainless steel and found that the formed weld

---

[*] Corresponding author.
*E-mail address:* zoujianglin1@163.com (J.L. Zou).

https://doi.org/10.1016/j.jmapro.2018.06.031
Received 28 March 2018; Received in revised form 15 June 2018; Accepted 19 June 2018

showed favorable anti-corrosion performance [13]. Gong et al performed gas tungsten arc welding (GTAW) on SAF2205 duplex stainless steel. After the addition of 2% $N_2$ in the protective atmosphere, the pitting sensitivity of welds was effectively restrained, the stability of passive film was improved and the adverse effects of welding on stress corrosion were reduced overall [14].

Many of research results have demonstrated that solution strengthening by nitrogen in micro-alloying can improve significantly the mechanical properties, fatigue strength and anti-corrosion performance of stainless steels. During laser welding, the partial pressure of metal vapor in the plasma/plume effectively reduces the partial pressure of $N_2$ in the protective atmosphere. Accordingly, the dissolution of nitrogen in the molten weld pool is far smaller than during traditional arc welding [9]. In addition, laser welding has a rapid cooling process, as a result of which, the weld pool has already solidified before the ionized and decomposed nitrogen can be dissolved in it. This also can reduce the dissolution of nitrogen in the weld to a certain degree. Bárta et al carried out $CO_2$ laser welding on duplex stainless steel and acquired welds with smooth surfaces and no welding defects under the protection of $N_2$. Moreover, the welds were comparable to those formed under the protection of pure Ar, and also exhibited better bending properties [15]. On the other hand, the content of austenite in the weld increased significantly from 24% to 56% [16]. However, the dissolution behavior of nitrogen in the weld, and the related distribution and existence states, still need further systemic study.

The present study employed a fiber laser and a $CO_2$ laser for conducting laser welding tests on austenitic stainless steel (SUS301L) plates with a thickness of 2 mm. Welds produced under different gas shielding conditions were compared systematically in terms of macro-appearance, microstructure, micro-hardness, tensile strength, nitrogen content in the weld as well as anti-corrosion performance. Finally, the dissolution and metallurgical behavior of nitrogen during these two lasers welding of stainless steel under nitrogen gas shielding were examined in depth.

## 2. Experimental materials and conditions

In this study, welding tests were conducted on austenitic stainless steel plates with a thickness of 2 mm, which were manufactured by cold rolling after solution treatment, and were composed of 71.25% Fe, 17.7% Cr, 7.15% Ni, 0.02% C, 1.08% Mn, 0.04% P, 0.003% S, 0.43% Si, and 0.2% N. In terms of strength, these stainless steel materials can be graded as special tensile (ST): the matrix has a tensile strength of 845 MPa and a yield strength of 480 MPa. A fiber laser (YLS-6000, IPG Photonics, America) and a $CO_2$ laser (Slab DC350, Rofin Co., Ltd., Germany) were used for laser welding in this study. The laser fiber had a focal length of 300 mm and the focus spot 0.3 mm in diameter, while the $CO_2$ fiber had a focal length of 300 mm and a focus spot diameter of 0.27 mm. The arrangement of devices in the welding tests is shown in Fig. 1. The stainless steel plates were welded by scanning welding, during which the protective gas was blown from the side, the laser power was set at 2 kW, the welding velocity was set at 1.5 m/min and the defocusing distance was 0. Using a gas mixer, the overall flow of the protective gas was set as 20 L/min and different mixtures of $N_2$ and Ar with different flow percentages (specifically, 100%$N_2$, 75%$N_2$ + 25%Ar, 50%$N_2$ + 50%Ar, 25%$N_2$ + 75%Ar and 100%Ar) were utilized for protection.

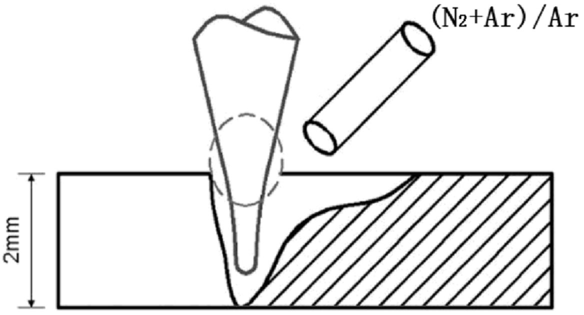

**Fig. 1.** Experimental layout of the ultra-narrow-gap laser conduction welding with filler wire.

After welding, the specimen first was cut along the cross-section and was then ground, polished and corroded. An optical microscope and a scanning electron microscope (SEM) were employed to observe the micro-morphology of the welds. An energy dispersive spectrometer (EDS) was used for component analysis and an X-ray diffractometer (XRD) was used for to analyze the phase constituents in the weld. The micro-hardness distribution of the weld joint was examined using a micro-hardness meter (FUTURE-TECH, Hitachi, Japan), during which a load with a magnitude of 100 g was applied for 15 s. Tensile tests were conducted on the U-shaped notches using an electro-hydraulic servo material tester (810, MTS Co., Ltd, America), for the sizes of tensile samples shown in Fig. 2.

The average nitrogen content in the weld was measured using an analyzer (ONH-2000, ELTRA Co., Ltd., Germany), while the content and existence form of nitrogen on the weld surface were detected using XPS (Thermo escalab 250 XI, America) and compared with the binding energy results for the fitting analysis. Specifically, monochromatic Al-Ka was used as the X-ray source (hv = 1486.6 eV). The power was set as 150 W, a beam spot with a diameter of 500 μm was used, and polluted carbon (C1s = 284.8 eV) was used for charge correction. The polarization curve for the weld surface was measured using an electrochemical analyzer (Biologic-VMP3, Claix Co., Ltd., France), and self-corrosion voltage and self-corrosion current were acquired through fitting, during which NaCl with a concentration of 3.5% was used, and the scanning velocity was set as 10 mV/s. The distribution of ferrite content in the weld's cross-section was observed using a Zeiss axiovert microscope. The nitrogen content at the center of the weld along the depth direction was measured using an EPMA electron probe (JXA-8320, Japan). Specifically, the nitrogen contents were measured every 100 μm from top to bottom; at each position, and the nitrogen content was measured 3–4 times for averaging.

## 3. Experimental results

### 3.1. Weld profiles and microstructure

The surface view and cross-section view of the welds after fiber laser welding and $CO_2$ laser welding under the protection of pure $N_2$ and pure Ar, respectively are summarized in Fig. 3. The welds appear well-formed, with smooth and continuous surfaces, and no spatters can be observed on either side of the welds. No obvious weld defects, such as undercutting or poor fusion, were evident. These observations were indicative of the stability of fiber laser welding and $CO_2$ welding under the protection of $N_2$ or Ar. Next, X-ray non-destructive inspection was performed, and different cross-sections of the welds were cut for observation. As shown in Fig. 3, no weld defects such as pores or cracks were observed. During the welding process, intensive laser energy was input from the upper surface of the weld and cooling was relatively slow, thereby forming a "nail-shaped" weld cross-section characterized by wide top and narrow bottom.

The microstructures of the welds at the center and around the fusion lines are shown in Figs. 4 and 5. By comparing the microstructures of the acquired welds under different protective atmospheres it can be concluded that $N_2$, as the protective gas in fiber laser welding or $CO_2$ laser welding processes, resulted in no significant detrimental effects on the formation and microstructures of the welds. The weld centers consist mainly of fine equiaxial dendritic crystals, while fine columnar crystals that are perpendicular to the boundary of the molten pool developed towards the weld center and were gathered around the fusion line. The difference at different positions of the weld in the